Materials Science Forum *Online: 2009-12-03*
ISSN: 1662-9752, Vol. 635, pp 63-68
doi:10.4028/www.scientific.net/MSF.635.63

X-ray Diffraction Reciprocal Space Mapping Study of Modulated Crystal Structures in 10M Ni-Mn-Ga Martensitic Phase

Yanling Ge[1a], Ilkka Aaltio[1b], Outi Söderberg[1c], Simo-Pekka Hannula[1d]

Department of Materials Science and Engineering, Helsinki University of Technology, P.O. Box 6200, FI-02015 TKK, Finland

[a]yanling.ge@tkk.fi, [b]ilkka.aaltio@tkk.fi, [c]outi.soderber@tkk.fi, [d]simo-pekka.hannula@tkk.fi

Keywords: Ni-Mn-Ga, X-ray diffraction (XRD), reciprocal space mapping (RSM).

Abstract. The 10M modulated crystal structure in Ni-Mn-Ga martensitic phase with about 0.5 MPa twinning stress, was studied by X-ray diffraction reciprocal space mapping (RSM). The experimental procedure is established for collecting large range of RSM with scattering planes inclined to the surface of specimen. The investigation focused on the superlattice reflections caused by the modulation, which always appeared in two <110> directions in bulk material. The distribution of two modulation domains varies with scattering locations.

Introduction

Ni-Mn-Ga magnetic shape memory (MSM) alloys belong to the new class of active materials exhibiting the giant magnetic field induced strain (MFIS) up to about 10 % [1-5]. These alloys have been investigated intensively for their versatile properties and potential applications [6-8].

Ni-Mn-Ga alloy has a Heusler $L2_1$-order cubic structure and it shows the martensitic transformation as well as magnetic transition from the paramagnetic state to the ferromagnetic one during cooling. There are three major types of martensitic crystal structures. The non-modulated martensite has a tetragonal structure with $c > a$ (when the lattice parameters c and a are given in the parent coordinates), which does not exhibit MSM effect due to high twinning stress needed to trigger the twin boundary motion and low magnetic stress, i.e. the stress yielded by the magnetic field due to the magnetic anisotropy. The modulated seven-layered martensite, 14M, has in average an orthorhombic structure showing the maximum MFIS of 10 %. The modulated five-layered martensite, 10M, has in average tetragonal lattice with $c < a$, and the maximum MFIS about 6% determined by the tetragonal distortion. Its twinning stress is much lower than the magnetic stress. The 10M martensite seems the one mostly studied of the above mentioned martensites [9-12]. In this type of martensite it is also easiest to obtain a single twin variant structure necessary for measurements and applications. However, even though this martensite type has been studied intensively, there are still unknown details concerning its crystal structure. Therefore, in the present study a new approach has been applied in order to clarify the fine details of the structure.

Reciprocal space mapping (RSM) is a recently developed state of art technique for data collection using X-ray diffraction techniques [13-14]. The detailed RSM can reveal more information about the state of crystal structure, such as defects, and relaxation. With variety of configurations of diffractometer, the RSM can be used to solve different microstructure problems, from low angle resolutions for enhanced intensities of poorly diffracting materials to high angle resolutions for very precise work. This method has been widely applied for the semiconductors having relatively perfect crystal structure. Ni-Mn-Ga alloy is an intermetallic compound, and its crystal structure is locally sensitive to any fluctuation of chemical composition. Therefore, comparison with semiconductors it is far from perfect. In the present work the reciprocal space mapping method is implemented and established to study the modulation structure of 10M martensite in an alloy which has twinning stress of 0.5 MPa. Since the modulation can occur in either one of <110> direction, there exists a interface between these two domains. The intensity

ratio for two modulation domain is related to their distribution. The distribution of this modulation in two <110> directions should shed a light to the quality of crystal and intrinsic defects.

Experimental procedure

The studied specimen with dimensions of 25 x 3 x 3 mm was fabricated by AdaptaMat Ltd. Its composition was $Ni_{50}Mn_{28}Ga_{22}$. This alloy exhibited martensitic transformation temperature T_M = 308 K and the respective reverse transformation T_A = 314 K. The twinning stress was about 0.5MPa.

The reciprocal space mapping was carried out with the PanAnalytic/Philips X'pert MRD diffractometer with $Co_{K\alpha}$ radiation. The Poly-capillary Lens with crossed slit collimator was set on the incident beam path. Iron filter was placed in the incident beam path to reduce the K_β spectra line. The divergence slit and axial slit were set with crossed slit collimator at 0.5mm. A parallel plate collimator of 0.27° was in the diffracted beam path as well as a mask acting as an axial slit in front of the detector. All texture measurements were made with a 2 mm mask.

The edges of the specimen were approximately parallel to the basic lattice vector of martensite. The specimen was in a single variant state obtained by magnetization along one of 3 mm edges. The specimen was mounted on the diffractometer with its *a* direction approximately along the Z direction of diffractometer, *c* along X direction, and *b* along Y direction. There is always slight misorientation due to inaccuracy in cutting or grinding. The orientation of the specimen was determined with the texture measurement. The texture measurements were made for four poles, (400), (620), (220) and (202) in order to obtain the precise orientation and to ensure that the specimen is in one variant state. Because the modulation lattice is along <110> direction, the available reciprocal space section for reveal the modulation reciprocal lattice points is from $(6\bar{2}0)$ to (400), or from (400) to (620). The precise orientations must be known in order to have all three reflections $(6\bar{2}0)$, (400) and (620) in one reciprocal lattice plane and set the range of RSM measurement. The orientation of specimen is visualized by stereo projection with CaRIne program.

Since $(6\bar{2}0)$, (400) and (620) have a common zone axis [001], when the [001] axis is aligned normal to the diffractometer plane, the detector can collect data from the area including all three reflections in reciprocal space. The orientation and lattice parameter is inserted in the unit cell information in X'pert DataCollector program. The reciprocal space map is selected to include the desired three reflections. The rotation angle phi (φ) and tilt angle psi (ψ) are calculated in the reciprocal space map. These values do not give the precise position for maximum intensity. Therefore, the manual scan should be used to optimize ω and 2θ, which will be used in the following texture measurement for the optimization of φ and ψ. These texture is measured for the poles (620), (400) and $(6\bar{2}0)$ with the step size 0.1° for both φ and ψ. Here, the offset for ω is used since the goal is to find the optimum φ and ψ for reciprocal space mapping alignment; this offset is selected so that the omega is half of two theta during the texture measurement. The optimized φ and ψ for the poles are different from each other, difference being as large as 0.8° for φ and 0.7° for ψ in one place in the specimen. This maybe because the diffraction condition is not the same for all three reflections. It is noted from the texture results that the deviation of 0.2° in both φ and ψ would miss the optimized peak in the reciprocal space mapping. Therefore, a compromise must be made in order to collect all three reflections in one map. The average position of phi and psi can be used with a large mask, 20 mm, to accept the large axial divergence, which could compensate for the difference in φ. The intensity in the map is measured and compared with the intensity from the texture results in order to check the validity of intensity in the RSM. A small range of RSM around the pole (400) includes four of the first order of superlattice points is collected with mask 2 mm. The intensity in this small map is again compared with the texture measurement for all four superlattice points.

Results and discussions

The orientation of the specimen was determined from the texture measurements of four poles (400), (620), (220) and (202) and visualized in stereo projection created with CaRine program, and shown in Fig. 1. Its mounting condition on the diffractometer and the lattice axis directions is marked schematically in Fig. 1. The (100) is tilted about 7° from the surface of specimen.

In Fig. 2, the texture measurements of ($6\bar{2}0$), (400) and (620) are shown. These texture measurements were made with ω offset for finding the optimized φ and ψ for RSM alignment. The compromised position for the three reflections was determined from these texture results and used for the RSM collection with the 20 mm mask, as shown in Fig. 3. All three main reflections together with the superlattice reflections are visible in the map. It is suggested that the 20 mm mask can accept more axial divergence of the diffracted beam to compensate the difference in the ψ angle.

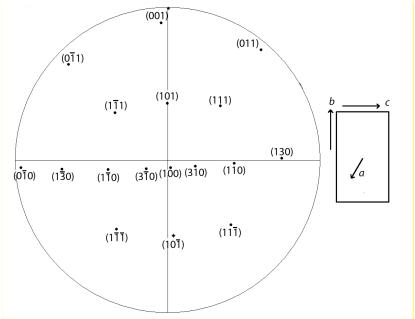

Fig. 1: The orientation of the specimen and its mounting condition on the diffractometer.

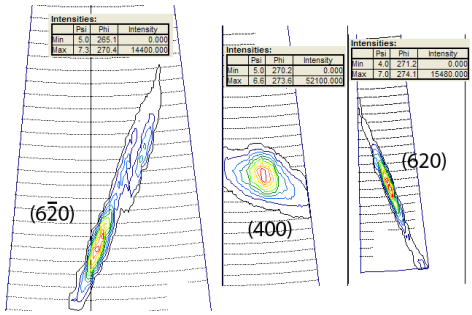

Fig. 2: The texture measurements with the omega offset of the three poles (400), (620) and ($6\bar{2}0$).

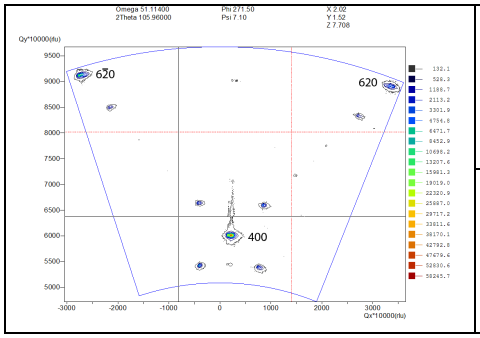

Pole	Intensity from texture	Intensity from RSM
620	15480	6080
$6\bar{2}0$	14400	19730
400	52100	63925

Fig. 3: The reciprocal space mapping with the 20 mm mask

By comparing the intensities from the texture in Fig. 2 and those from RSM in Fig. 3, the intensity of the (620) is only one third of that of the ($6\bar{2}0$) in RSM. However, in the texture figure, the intensity of the (620) is close to that of the ($6\bar{2}0$). The observed disparity is due to the 2.6° φ angle difference between the texture maximum position and the RSM φ setting. This suggests that one could use the large axis slit to reveal the modulation structure, but then the intensities measured in this map do not correspond to the maximum intensity. It is also demonstrated that the large range of reciprocal space map is difficult to collect. It is worth to note that the co-occurrence of superlattice in two directions <110>, in Fig. 3, clearly indicate the existence of twinned domains with modulation direction normal to each other [12] since the modulation occurs in only one of <110> direction.

The above results suggest that reducing the range of the map will decrease the difference of φ and ψ angles between reflections. Now, in Fig. 4 two maps are collected around the pole (400) including four the first order superlattice points with the 20 mm and 2 mm mask, respectively. Also, the respective texture measurements are shown in Fig. 4. The intensities of all four superlattice points are measured from two RSMs and compared with the texture measurements in Table 1.

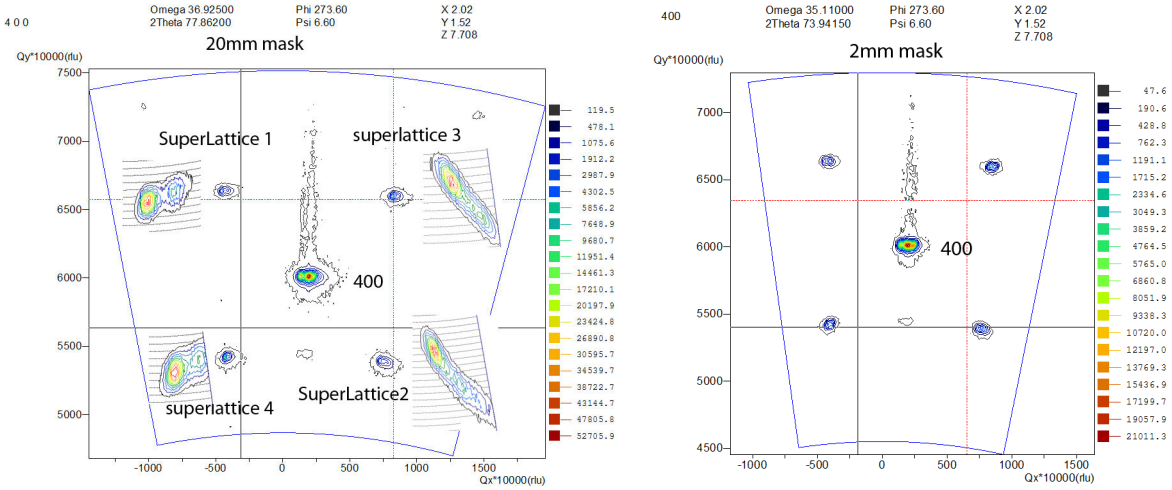

Fig. 4: Two RSMs of the pole (400) measured with the 20 mm and 2 mm mask, respectively, and the texture measurements (insets next to reciprocal lattice point) of four of the first order superlattice points.

It is noted that in the RSM the 20 mm mask increases the intensity of the (400) reflection more than twice than when the 2 mm mask is used. The detailed intensities and coordinates of the reflections in the reciprocal space are listed in Table 1. Superlattice points 1 and 2 are along the $[1\bar{1}0]$* direction and the points 3 and 4 are along the [110]* direction. In the case of the points 1 and 2, the 20 mm mask in the RSM gives in addition to the intensity close to that in the texture measurement, also the ω and 2θ angular values that are close to the optimized values obtained in the manual scan before the texture measurement. For the superlattice points 3 and 4, the 2 mm mask gives better the angular values of the ω and 2θ, but the intensity of the point 4 is much lower than it should be. Here, the 20 mm mask gives a comparable intensity with the texture measurement while the ω and 2θ values are to some extent deviated from the texture measurement. Those differences are due to the optimized positions in the texture, the φ and ψ, for the points 3 and 4, which are more away from the optimized 400 position, the φ difference being 0.3° and the ψ deviation of 0.2°. These results show that the structure smearing effect is stronger than the probe size, thus, the large axis divergence is suitable for small range of the RSM providing relative good intensity together with the ω and 2θ.

Table 1: The coordinates and intensities from the texture and the RSM measurements.

		ω	2θ	phi	psi	intensity
Superlattice point 1 on the left-upper of 400	Texture 2mm mask	45.625	83.386	273.8	6.5	3770
	RSM with 2 mm mask	45.110	83.3415	273.6	6.6	1610
	RSM with 20 mm mask	45.625	83.462	273.6	6.6	3695
Superlattice point 2 on the right-lower of 400	Texture	25.320	65.960	273.4	6.6	4160
	RSM 2 mm mask	24.910	65.9415	273.6	6.6	2440
	RSM 20 mm mask	25.325	65.862	273.6	6.6	4055
Superlattice point 3 on the right-upper of 400	Texture	34.499	83.377	273.4	6.4	4720
	RSM 2 mm mask	34.510	83.3415	273.6	6.6	2785
	RSM 20 mm mask	34.625	83.462	273.6	6.6	6935
Superlattice point 4 on the left-lower of 400	Texture	37.416	65.912	273.9	6.4	7600
	RSM 2 mm mask	37.410	65.9415	273.6	6.6	2485
	RSM 20 mm mask	37.525	65.862	273.6	6.6	9005

The double peak is observed in all the reflections, the basic (400) reflection as well as the superlattice points. The double peaks are aligned along the omega axis, while the two theta values are nearly same, shown in Fig. 5. The angle difference is about 0.6°. It means the presence of two variants which rotated 0.6° along [010]. It also could be considered as a-b twinning which is due to the small rotation of habit plane (110) from parent phase. The RSMs in Fig. 5 is collected from two locations in the specimen, which is 9.5 mm apart along Y direction. The distribution of modulation domains should propositional to ratio of superlattice intensity of corresponding order. The ratio is from 0.5 to 1 calculated from Table 1. First the different ratio from Table 1 means the shape and position of reciprocal lattice point need to be further investigated. 3-D RSM should reveal more information about the lattice shape, in which RSM is collected with a small change in ψ. If we compare the ratio from Fig. 5 of two RSMs, it is clear the ratio is change with scattering locations too. This is indicated that the modulation domains are unevenly distributed, the further investigation is needed to clarity whether this distribution related with some intrinsic defects.

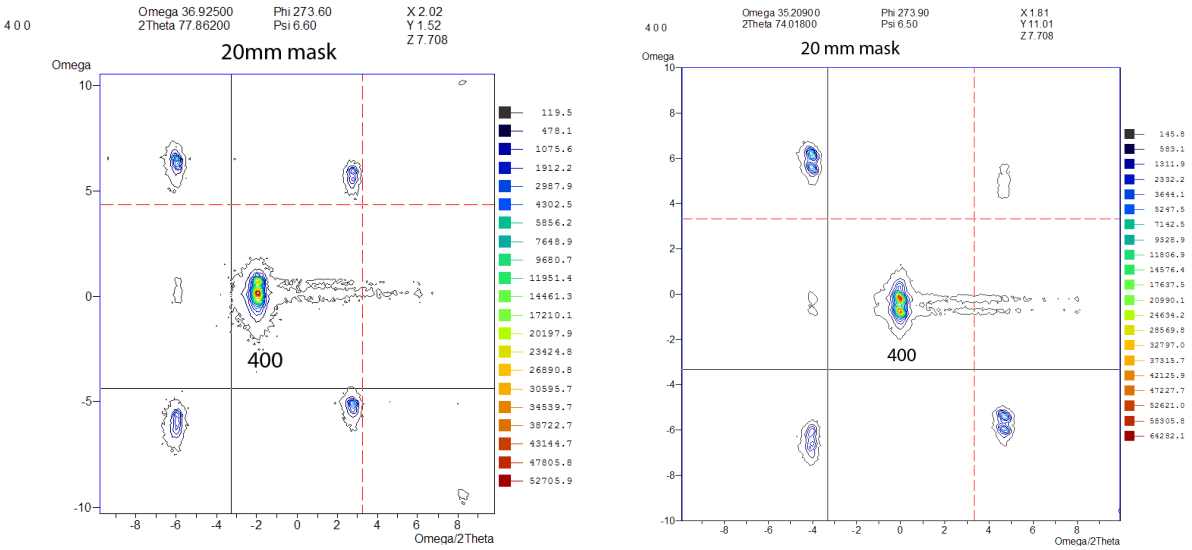

Fig. 5: The two RSM made from two locations on the specimen, 9.5mm apart along Y direction.

Conclusions

Due to the intrinsic nature of intermetallic Ni-Mn-Ga compounds, i.e. the crystal structure is far from the perfect one, their single crystal orientation is usually deviated several degrees from the low index crystal plane, obtaining high quality reciprocal space mapping is much more difficult than with the semiconductors. The careful aligning procedure is needed to ensure the desired reflections that could be collected in one map. The large axial slit is proved to be helpful to compromise the local differences in the scattering conditions to obtain reliable intensity to some extent in the RSM. This method is demonstrated with an alloy showing modulation in both two <110> directions. The double peaks revealed in RSM in all of the reflections could be due to the mosaic structure or the monoclinicity of the average structure. The modulation domains are distributed unevenly in the specimen.

Acknowledgements

The Academy of Finland is acknowledged for funding the post-doc project of Yanling Ge. Authors would like to thank AdaptaMat Oy for supplying the sample and Ms. Raisa Niemi for magnetic susceptibility measurement.

References

[1] K. Ullakko, J. K. Huang, C. Kantner, R. C. O'Handley and V. V. Kokorin: Appl. Phys. Lett. Vol. 69 (1996), p119.

[2] V.A. Chernenko, E. Cesari, V.V. Kokorin and I.N. Vitenko: Scripta Met. Mat. Vol. 33 (1995) p1239.

[3] O. Heczko, A. Sozinov and K. Ullakko: IEEE Trans. Magn. Vol. 36 (2000), p3266.

[4] S.J. Murray, M. Marioni, S.M. Allen, R.C. O'Handley and T.A. Lograsso: Appl. Phys. Lett. Vol. 77 (2000), p886.

[5] A. Sozinov, A.A. Likhachev, N. Lanska and K. Ullakko: Appl. Phys. Lett. Vol. 80 (2002), p1746.

[6] I. Aaltio, O. Heczko, O. Söderberg and S.-P. Hannula: Magnetically activated ferromagnetic shape memory alloys, in Smart Materials, edited by Mel Schwartz, CRC Press Taylor & Francis Group, Boca Raton FL USA, (2009).

[7] O. Söderberg, Y. Ge, I. Aaltio, O. Heczko and S.-P. Hannula: Mat. Sci. Eng. A Vol. 481-482 (2008), p80.

[8] S.A. Wilson, R.P.J. Jourdain, Q. Zhang, R.A. Dorey, C.R. Bowen, M. Willander, Q. Ul Wahab, S.M. Al-hilli, O. Nur, E. Quandt, C. Johansson, E. Pagounis, M. Kohl, J. Matovic, B. Samel, W. van der Wijngaart, E.W.H. Jager, D. Carlsson, Z. Djinovic, M. Wegenerp, C. Moldovanm, R. Iosubm, , E. Abadn, M. Wendlandto, C. Rusug and K. Persson, Mat. Sci. Eng. R Vol.56 (2007), p. 1.

[9] V.V. Martynov and V.V. Kokorin, J. Phys. (France) III Vol. 2 (1992), p739.

[10] J. Pons, V.A. Chernenko, R. Santamarta and E. Cesari: Acta Mater. Vol. 48 (2000), p3027.

[11] L. Righi, F. Albertini, G. Calestani, L. Pareti, A. Paoluzi, C. Ritter, P.A. Algarabel, L. Morellon and M.R. Ibarra: J. Sol. Stat. Chem. Vol. 179 (2006), p3525.

[12] Y. Ge, H. Jiang, A. Sozinov, O. Söderberg, N. Lanska, J. Keränen, E.I. Kauppinen, V.K. Lindroos and S.-P. Hannula Mat. Sci. Eng. A: Vol. 438-440 (2006), p961.

[13] P.F. Fewster:X-Ray Scattering from Semiconductors (Imperial College Press, London 2003)

[14] P.F. Fewster: Critical Rev. Solid State Mater. Sci. Vol. 22 (1997), p69